Spontaneous symmetry breaking in totally asymmetric simple exclusion processes on two intersected lattices

2008 J. Phys. A: Math. Theor. 41 035003

(http://iopscience.iop.org/1751-8121/41/3/035003)

J. Phys. A: Math. Theor. **41** (2008) 035003 (17pp) doi:10.1088/1751-8113/41/3/035003

Spontaneous symmetry breaking in totally asymmetric simple exclusion processes on two intersected lattices

Yao-Ming Yuan[1], **Rui Jiang**[1], **Ruili Wang**[2], **Qing-Song Wu**[1] **and Jin-Qiu Zhang**[1]

[1] School of Engineering Science, University of Science and Technology of China, Hefei, Anhui 230026, People's Republic of China
[2] Institute of Information Sciences and Technology, Massey University, New Zealand

Received 20 September 2007, in final form 22 November 2007
Published 4 January 2008
Online at stacks.iop.org/JPhysA/41/035003

Abstract

This paper studies totally asymmetric simple exclusion processes (TASEPs) on two intersected lattices. Three different models are introduced: model A for molecular motor motion, and models B and C for vehicle traffic. Extensive Monte Carlo simulations are carried out. Phase diagrams and density profiles of the three models are investigated. It is shown that phase diagrams of all the three models are divided into three regions. The phase boundaries are calculated by an approximate mean-field approach. It is found that the analytic solutions are in good agreement with the results of Monte Carlo simulations. For models B and C, spontaneous symmetry breaking is identified. The particle density histograms and qualitative domain-wall explanation are presented to describe the spontaneous symmetry breaking phenomenon. Finally, in model C, the effect of lane-changing probability p on spontaneous symmetry breaking is investigated. A threshold of p for the occurrence of symmetry breaking is obtained.

PACS numbers: 05.70.Ln, 02.50.Ey, 05.60.Cd

(Some figures in this article are in colour only in the electronic version)

1. Introduction

In recent years, asymmetric simple exclusion processes (ASEPs), which are discrete non-equilibrium models that describe the stochastic dynamics of multi-particle transport along one-dimensional lattices, have attracted the interests of physicists because it is an important tool for understanding complex non-equilibrium phenomena [1–3]. In ASEPs, each lattice site can be either empty or occupied by a single particle. Particles interact only through hard-core exclusion potential. ASEPs was first introduced in 1968 for describing the kinetics of biopolymerization [4] and then have been applied successfully to analyze surface growth [5, 6], gel electrophoresis [7], diffusion through membrane channels [8], protein synthesis [9–11], dynamics of motor proteins moving along rigid filaments [12], traffic flow [13], etc.

The simplest limit of an ASEP, which is called the totally asymmetric simple exclusion processes (TASEP), is that particles can only move in one direction. The exact solutions of TASEP exist [14, 15]. In this paper, we consider random sequential update rules, i.e., at each time step we randomly choose a site on lattice to follow its dynamics. In this case, three stationary phases exist, specified by the processes at the entrance, at the exit and in the bulk of the system. Denote the injection and extraction rates at the entrance and exit by α and β, respectively. For $\alpha < \beta$ and $\alpha < 0.5$, the system is found in a low-density (LD) entry limited phase with the particle current and bulk density

$$J_{\mathrm{LD}} = \alpha(1-\alpha) \qquad \text{and} \qquad \rho_{\mathrm{bulk,LD}} = \alpha. \tag{1}$$

For $\alpha > \beta$ and $\beta < 0.5$, the system is in a high-density (HD) exit limited phase with the particle current and bulk density

$$J_{\mathrm{HD}} = \beta(1-\beta) \qquad \text{and} \qquad \rho_{\mathrm{bulk,HD}} = \beta. \tag{2}$$

And for $\alpha > 0.5$ and $\beta > 0.5$ the system is determined by processes in the bulk, and we have a maximal-current (MC) phase with

$$J_{\mathrm{MC}} = 0.25 \qquad \text{and} \qquad \rho_{\mathrm{bulk,MC}} = 0.5. \tag{3}$$

In order to analyze more realistic phenomena, a number of different extensions of ASEPs have been proposed, including particles occupy more than one lattice site [9, 16], disorders effect in the bulk [17–21], particle moving in system with periodically varying sitewise disorder [22], combination of random particles creation and annihilation [23], multi-lane extensions [24–29], allowance of long-range hopping [30] and so on.

Many non-equilibrium behaviors such as boundary induced phase transition, the unusual dynamical scaling and spontaneous symmetry breaking have been observed in ASEPs. One of the most intriguing phenomena is symmetry breaking that the microscopic symmetric dynamic rules lead to the occurrence of macroscopic asymmetric stationary states for some sets of parameters. The first model that exhibits spontaneous symmetry breaking was proposed in 1995, known as the 'bridge model' [31] where two species of particles move in opposite directions. Following the work of 'bridge model', symmetry breaking has been studied in detail in many other works [32–38].

This paper studies situations arising when two channels intersect at a crossing point, which is widely observed either in molecular motor motion or vehicle traffic. To our knowledge, ASEPs on two one-dimensional roads with a crossing have been studied only under periodic boundary condition and with parallel update rules [39]. In this paper, we investigate TASEPs on two one-dimensional lattices with an intersection under open boundary condition. The lattices are sketched in figure 1(*a*). Two one-dimensional lattices with equal length $2L+1$ intersect at site c. Lattice 1 is in the horizontal direction and lattice 2 is in the vertical direction. Therefore, the lattices are divided into four segments by site c, as shown in figure 1(*b*). The sites are numbered as follows: segment I corresponds to site $1 \rightarrow L$, segment II corresponds to site $L+2 \rightarrow 2L+1$, segment III corresponds to site $2L+2 \rightarrow 3L+1$, segment IV corresponds to site $3L+2 \rightarrow 4L+1$ and site c corresponds to site $L+1$.

The study may be relevant for both molecular motor motion and vehicle traffic. We present three different models. Model A is for molecular motor motion. In molecular motor motion, the filaments where molecular motors travel may be crossed with each other. When

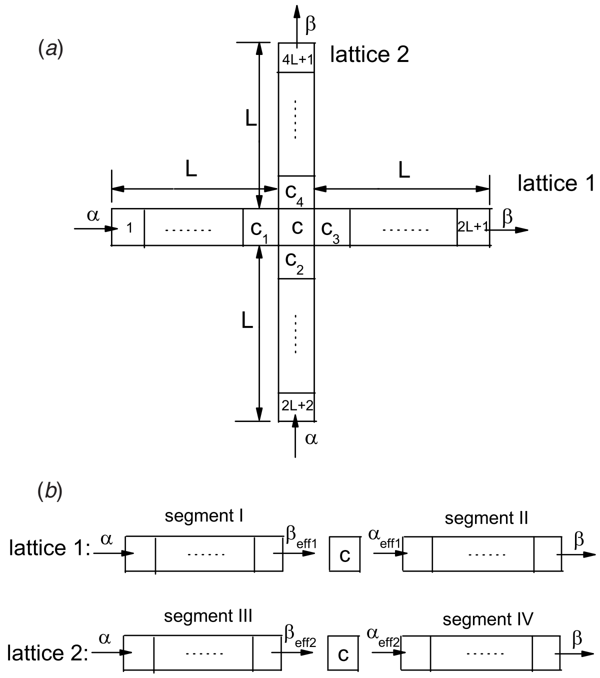

Figure 1. (*a*) The sketch of two one-dimensional lattices with crossing. (*b*) Each lattice is divided into two segments by site *c*.

the molecular motors arrive at the intersection, they may go to each of the two filaments. Thus, the molecular motors can be considered as no pre-defined destination. Models B and C are for vehicle traffic. In model B, the drivers know where the destination is and do not change the destination. In model C, drivers might change the destination at the intersection.

Extensive simulations are carried out. In all the simulations, we set $L = 1000$ unless otherwise mentioned. The phase diagrams and density profiles of all the three models are investigated in detail and interesting phenomena are observed and explained.

The paper is organized as follows. Sections 2–4 present the model rules, simulation results and results analysis of models A, B and C, respectively. Finally, the conclusion is given in section 5.

2. Model A

2.1. Model rules

In this section, the update rules of model A are introduced. Random update rules of TASEP are adopted. Note that the particles (corresponding to molecular motors here) do not have a pre-defined destination in this model. In an infinitesimal time interval d*t*, site *i* is chosen randomly ($1 \leqslant i \leqslant 4L + 1$).

- If $i = 1$ (entrance of lattice 1) or $i = 2L + 2$ (entrance of lattice 2), a particle is inserted into site 1 or $2L + 2$ with rate α provided the site is empty. If site 1 or $2L + 2$ is occupied, the particle moves to site $i + 1$ with rate 1 provided the site $i + 1$ is empty.

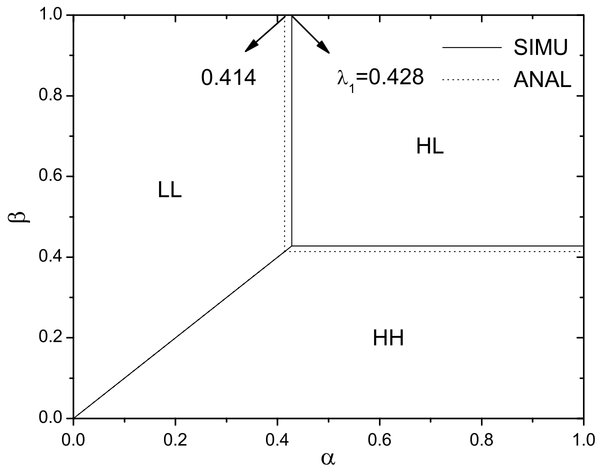

Figure 2. The phase diagram of model A related to α and β. The solid line is from Monte Carlo simulations and the dot line is from the mean-field approximation.

- If $i = 2L + 1$ (exit of lattice 1) or $i = 4L + 1$ (exit of lattice 2) and the site is not empty, the particle is removed with rate β.
- If $1 < i < L+1$ (segment I), or $L+1 < i < 2L+1$ (segment II), or $2L+2 < i < 3L+1$ (segment III), or $3L+2 \leqslant i < 4L+1$ (segment IV) and the site is occupied, the particle moves to site $i+1$ with rate 1 provided the site $i+1$ is empty. If $i = 3L+1$ (exit of segment III) and the site is occupied, the particle moves to site c with rate 1 provided the site c is empty.
- If $i = L+1$ (site c) and the site is occupied,
  - the particle moves to site c_3 with rate 1 provided the site c_3 is empty and the site c_4 is occupied,
  - the particle moves to site c_4 with rate 1 provided the site c_4 is empty and the site c_3 is occupied,
  - the particle moves to site c_3 with rate 0.5 and site c_4 with rate 0.5 provided both sites c_3 and c_4 are empty.

2.2. *Simulation results*

This section presents the simulation results of model A. The phase diagram related to α and β is shown in figure 2. The phase diagram can be classified into three regions, and the situations are always symmetric on both lattices. When $\alpha < \lambda_1 \approx 0.428$ and $\alpha < \beta$, both of the two segments of each lattice are in the low-density phase, i.e., the system is in the phase LL, as shown in figure 3(*a*). The bulk densities of all the four segments are equal and all equal to α.

When $\beta < \lambda_1 \approx 0.428$ and $\beta < \alpha$, the system is in the phase HH, as shown in figure 3(*b*). The bulk densities of all the four segments are equal and all equal to $1-\beta$.

When $\alpha > \lambda_1 \approx 0.428$ and $\beta > \lambda_1 \approx 0.428$, the system is in the phase HL. The bulk densities of segments I and III are equal and both equal to $1-\lambda_1$ and that of segments II and IV are λ_1.

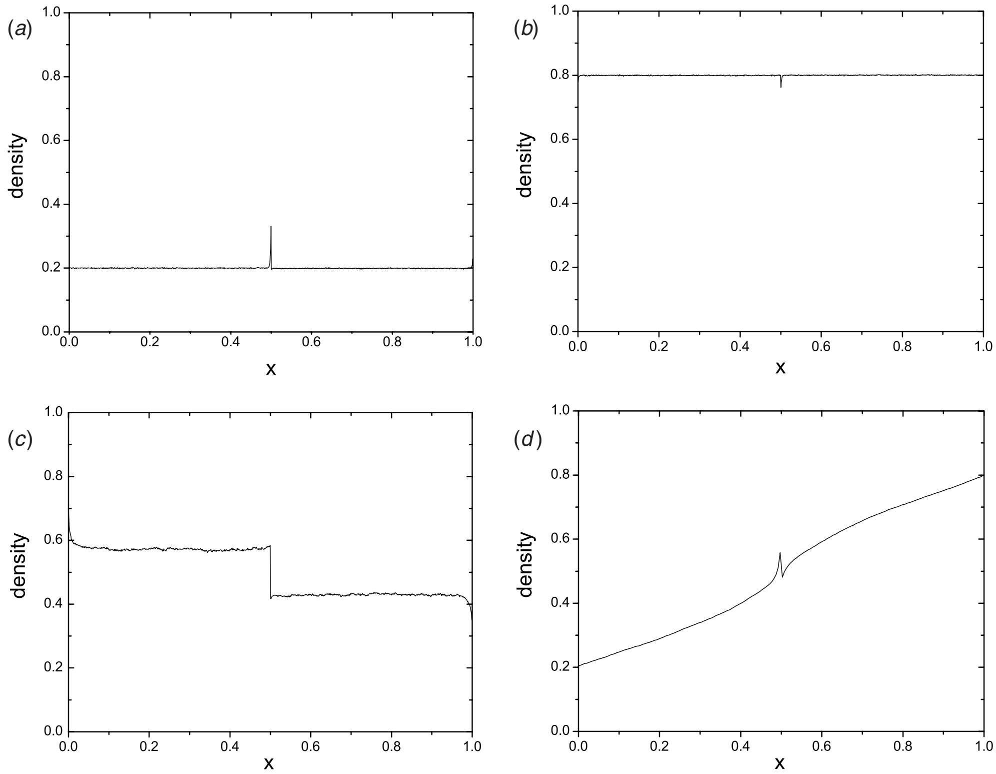

Figure 3. The density profiles of model A corresponding to different phases. Due to symmetry of the results, only density profiles of one lattice are shown. (*a*) $\alpha = 0.2$ and $\beta = 0.7$; (*b*) $\alpha = 0.7$ and $\beta = 0.2$; (*c*) $\alpha = 0.8$ and $\beta = 0.7$; (*d*) $\alpha = 0.2$ and $\beta = 0.2$, $L = 100$.

2.3. Results analysis

Next we present the approximate stationary solutions of model A by using the method proposed in [20]. As illustrated in figure 1(*b*), four segments are divided and each segment can be regarded as a lattice of original single-channel TASEP. The extraction rates of segments I and III are denoted by β_{eff1} and β_{eff2}, and the injection rates of segments II and IV are denoted by α_{eff1} and α_{eff2}, respectively. Due to the symmetry of the system and the symmetric results by simulations, all the properties in both lattices should be identical, i.e., $\beta_{\text{eff1}} = \beta_{\text{eff2}}$ and $\alpha_{\text{eff1}} = \alpha_{\text{eff2}}$. Their values are as follows:

$$\begin{aligned} &\beta_{\text{eff1}} = \beta_{\text{eff2}} = \beta_{\text{eff}} = 1 - \rho_c, \\ &\alpha_{\text{eff1}} = \alpha_{\text{eff2}} = \alpha_{\text{eff}} = \rho_c\left[\rho_{c_4} + 0.5\left(1 - \rho_{c_4}\right)\right] = 0.5\rho_c\left(1 + \rho_{c_4}\right). \end{aligned} \tag{4}$$

When the lattice is in the phase LL, we have

$$\begin{cases} \alpha < 0.5 & \text{and} \quad \alpha < \beta_{\text{eff}} \\ \alpha_{\text{eff}} < 0.5 & \text{and} \quad \alpha_{\text{eff}} < \beta. \end{cases} \tag{5}$$

Let us denote the fluxes of segments I and II by J_I and J_{II}, respectively. From $J_I = J_{II}$ and equation (1), we obtain $\rho_c = \frac{2\alpha}{1+\rho_{c_4}}$. And because segment IV is in the LD phase, $\rho_{c_4} = \alpha$.

Thus, $\rho_c = \frac{2\alpha}{1+\alpha}$. From equation (5), we obtain $\alpha < \beta_{\text{eff}} = 1-\rho_c = 1-\frac{2\alpha}{1+\alpha}$ and $\alpha_{\text{eff}} = \alpha < \beta$. Thus, the lattice is in the LL phase when the following conditions are satisfied:

$$\begin{cases} \alpha < \sqrt{2}-1 \\ \alpha < \beta. \end{cases} \tag{6}$$

Similarly, if the lattice is in the phase HH, then

$$\begin{cases} \beta_{\text{eff}} < 0.5 & \text{and} \quad \alpha > \beta_{\text{eff}} \\ \beta < 0.5 & \text{and} \quad \alpha_{\text{eff}} > \beta \end{cases} \tag{7}$$

should be satisfied. From $J_I = J_{II}$ and equation (2), we obtain $\beta_{\text{eff}} = \beta$, which leads to $\rho_c = 1-\beta$. Similarly, from $\alpha_{\text{eff}}\left(1-\rho_{c_4}\right) = \beta(1-\beta)$, we obtain $\rho_{c_4} = \sqrt{1-2\beta}$. Substituting these expressions into equation (7), we obtain the condition of the existence of the phase HH on a lattice:

$$\begin{cases} \beta < \sqrt{2}-1 \\ \beta < \alpha. \end{cases} \tag{8}$$

When the lattice is in the phase HL, then

$$\begin{cases} \beta_{\text{eff}} < 0.5 & \text{and} \quad \alpha > \beta_{\text{eff}} \\ \alpha_{\text{eff}} < 0.5 & \text{and} \quad \alpha_{\text{eff}} < \beta \end{cases} \tag{9}$$

should be satisfied. And from $J_I = J_{II}$ and equations (1) and (2), we obtain $\beta_{\text{eff}}(1-\beta_{\text{eff}}) = \alpha_{\text{eff}}(1-\alpha_{\text{eff}})$, which leads to $\beta_{\text{eff}} = \alpha_{\text{eff}}$ or $\alpha_{\text{eff}} + \beta_{\text{eff}} = 1$. Substituting the expressions of α_{eff} and β_{eff} into $\alpha_{\text{eff}} + \beta_{\text{eff}} = 1$, we obtain $1 - \rho_c + 0.5\rho_c\left(1+\rho_{c_4}\right) = 1$, which leads to $\rho_{c_4} = 1$. However, it is conflicted with that segment IV is in the phase LD. Thus, $\beta_{\text{eff}} = \alpha_{\text{eff}}$ should be satisfied. Substituting the expressions of α_{eff} and β_{eff} into $\beta_{\text{eff}} = \alpha_{\text{eff}}$, we obtain

$$0.5\rho_c\left(1+\rho_{c_4}\right) = 1-\rho_c. \tag{10}$$

Since segment IV is in low density, we have

$$\rho_{c_4} = \alpha_{\text{eff}}. \tag{11}$$

From the above two equations and equation (4), ρ_{c_4} could be obtained, $\rho_{c_4} = 1-\rho_c = \sqrt{2}-1$. After substituting this result into equation (9), the conditions of the existence of the phase HL on a lattice are as follows:

$$\begin{cases} \alpha > \sqrt{2}-1 \\ \beta > \sqrt{2}-1. \end{cases} \tag{12}$$

As shown in figure 2, the approximate stationary solutions are in good agreement with the simulation results. Finally, we would like to mention $\alpha = \beta < \sqrt{2}-1$ corresponds to a line of phase transition between phases LL and HH. Thus, a linear density profile exists except near site c (see figure 3(*d*)).

3. Model B

3.1. Model rules

Different from model A, the particles (corresponding to cars in vehicle traffic) in model B have a pre-defined destination. There are four types of particles: type 1 enters from site 1 and leaves from site $2L+1$; type 2 enters from site 1, changes direction at site c and leaves from site $4L+1$; type 3 enters from site $2L+2$ and leaves from site $4L+1$; type 4 enters from site $2L+2$, changes direction at site c and leaves from site $2L+1$.

Random update is also adopted and a random site i is chosen during an infinitesimal time interval dt.

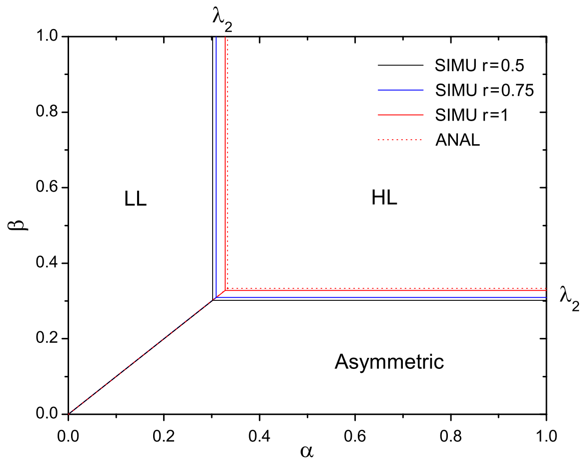

Figure 4. The phase diagram of model B related to α and β. Solid lines are from the Monte Carlo simulation results with $r = 1$, 0.75 and 0.5 and the red dot line is from the approximate mean-field approach.

- If $i = 1$ (entrance site of lattice 1) and the site is empty, a particle is inserted into the site with rate α. The particle is of type 1 with probability r, and of type 2 with probability $1 - r$. If the site is occupied, the particle will move to site $i + 1$ with rate 1 provided the site $i + 1$ is empty. Similarly, if $i = 2L + 2$ (entrance site of lattice 2) and the site is empty, a particle is inserted into the site with rate α. The particle is of type 3 with probability r, and of type 4 with probability $1 - r$. If the site is occupied, the particle will move to site $i + 1$ with rate 1 provided the site $i + 1$ is empty.
- If $i = 2L + 1$ (exit site of lattice 1) or $i = 4L + 1$ (exit site of lattice 2) and the site is occupied, the particle is removed with rate β.
- If $1 < i < L + 1$ (segment I), or $L + 1 < i < 2L + 1$ (segment II), or $2L + 2 < i < 3L + 1$ (segment III), or $3L + 2 \leqslant i < 4L + 1$ (segment IV) and the site is occupied, the particle moves to site $i + 1$ with rate 1 provided the site $i + 1$ is empty. If site $3L + 1$ (exit site of segment III) is chosen and the site is occupied, the particle moves to site c provided the site c is empty.
- If site $i = L + 1$ (site c) is chosen,
  - if the site is occupied by particle of type 1 or 4, the particle moves to site c_3 with rate 1 provided the site c_3 is empty, independent of the status of the site c_4,
  - if the site is occupied by particle of type 2 or 3, the particle moves to site c_4 with rate 1 provided the site c_4 is empty, independent of the status of the site c_3.

3.2. Simulation results

First, we focus on the phase diagram as shown in figure 4. Due to the symmetry of model rules, we restrict ourselves to the case $r \geqslant 0.5$.[3] It is found that the phase diagram is divided into three regions.

When $\alpha < \lambda_2$ and $\alpha < \beta$, the system is in the phase LL, as shown in figure 5(*a*). The bulk densities of all the four segments are equal and all equal to α, independent of r.

[3] For example, when $r = 0$, the situation is identical to that of $r = 1$ provided we assume lattice 1 consists of segments I and IV and lattice 2 consists of segments II and III.

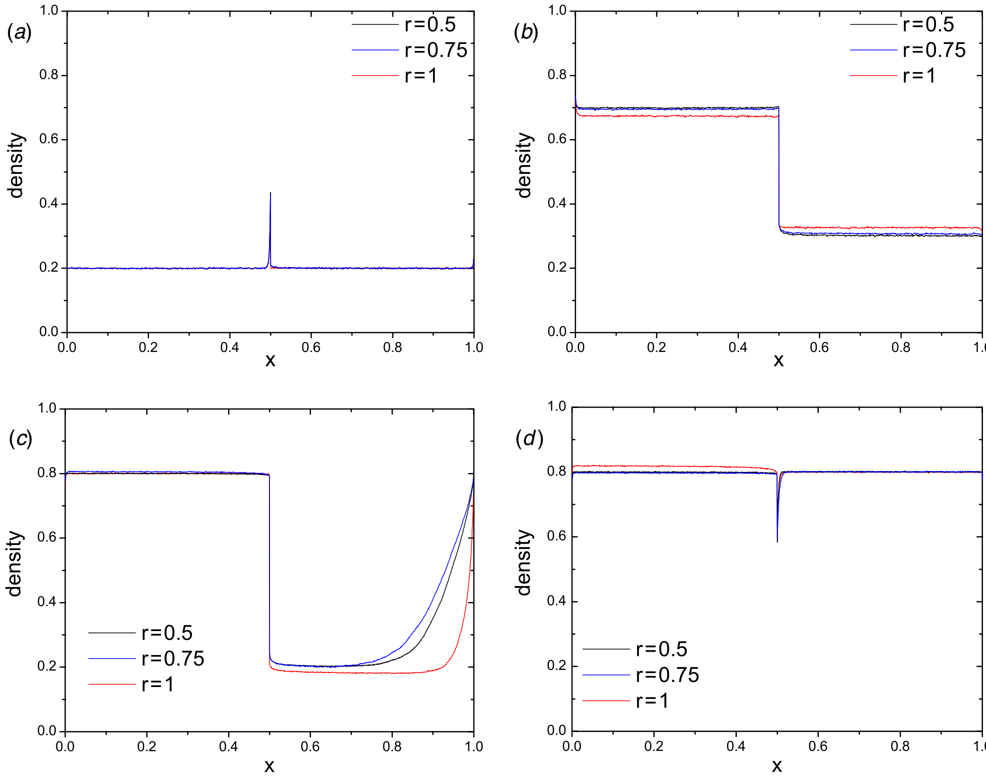

Figure 5. The density profiles of model B corresponding to different phases with different value of r. (a) $\alpha = 0.2$ and $\beta = 0.7$; (b) $\alpha = 0.8$ and $\beta = 0.7$; (c) $\alpha = 0.7$ and $\beta = 0.2$ of lattice 1; (d) $\alpha = 0.7$ and $\beta = 0.2$ of lattice 2.

When $\alpha > \lambda_2$ and $\beta > \lambda_2$, the system is in the phase HL, as shown in figure 5(b). The bulk densities of segments I and III are equal and both equal to $1 - \lambda_2$ and that of segments II and IV are λ_2.

When $\beta < \lambda_2$ and $\beta \leqslant \alpha$, it is very interesting to find that spontaneous symmetry breaking occurs in this region, as shown in figures 5(c) and (d). The bulk densities of the two segments on one lattice equals $1 - \beta$. On the other lattice, the bulk density on the downstream segment is slightly lower than β and that on the upstream segment is slightly larger than $1 - \beta$. Note that the fluxes on both lattices differ only slightly, which is rather different situation than in the 'bridge model' [31], where both densities and fluxes differ macroscopically. Moreover, in our simulation, we found that the difference of fluxes on both lattices essentially does not vary with system size.

Following [36], we also investigate the particle density histograms $P_L(\rho_1, \rho_2)$, where ρ_1 and ρ_2 are instantaneous densities of particles in segments II and IV. Figure 6 shows the particle density histogram with $\alpha = 0.7$, $\beta = 0.2$ and $r = 1, 0.75$ and 0.5. It is shown that the peaks are off the diagonal, which means that symmetry breaking occurs.

To demonstrate the spontaneous symmetry breaking, the flipping times between the two states of the broken symmetry phase in a finite-sized system are studied. Figure 7(a) shows the time evolution of the density difference between segments II and IV in an asymmetric phase. Flips between the two symmetry related states are clearly seen.

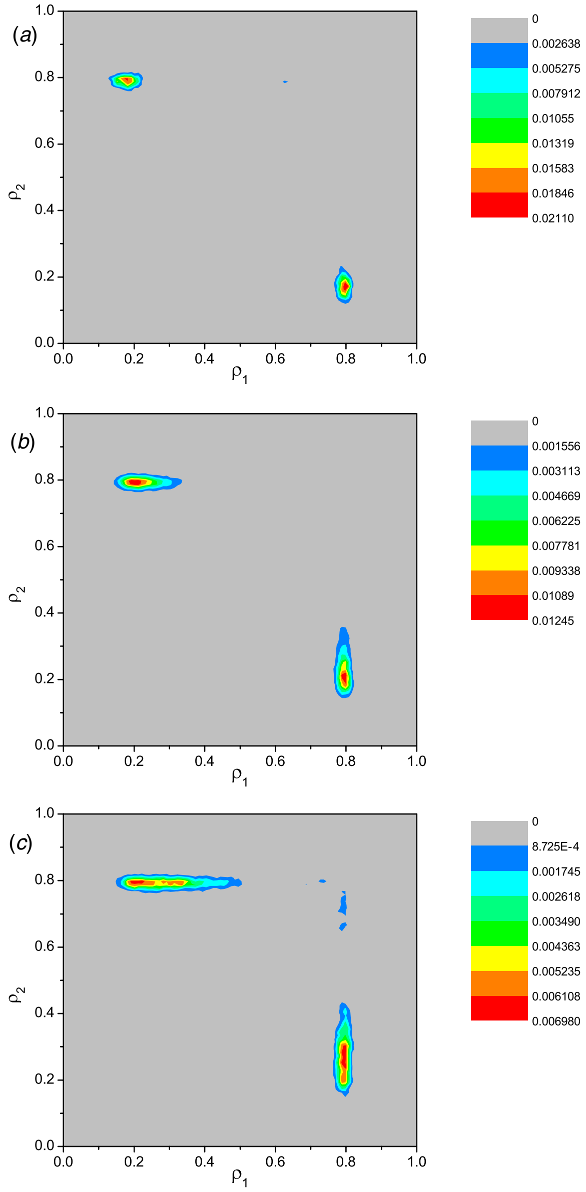

Figure 6. The density histograms of model B corresponding to the asymmetric phase with different value of r. ρ_1 denotes the instantaneous densities of segment II and ρ_2 denotes the instantaneous densities of segment IV. $\alpha = 0.7$ and $\beta = 0.2$. (*a*) $r = 1$; (*b*) $r = 0.75$; (*c*) $r = 0.5$.

To evaluate the characteristic flipping time scale τ, we averaged the density difference over many runs, starting from the configuration that all sites on segment II are occupied and all sites on segment IV are empty. This average decays as $e^{-t/\tau}$ and thus yields τ (see, e.g., figure 7(*b*)). The time scale versus L is shown in figure 8. It can be seen τ grows exponentially with the L, which indicates spontaneous symmetry breaking does exist.

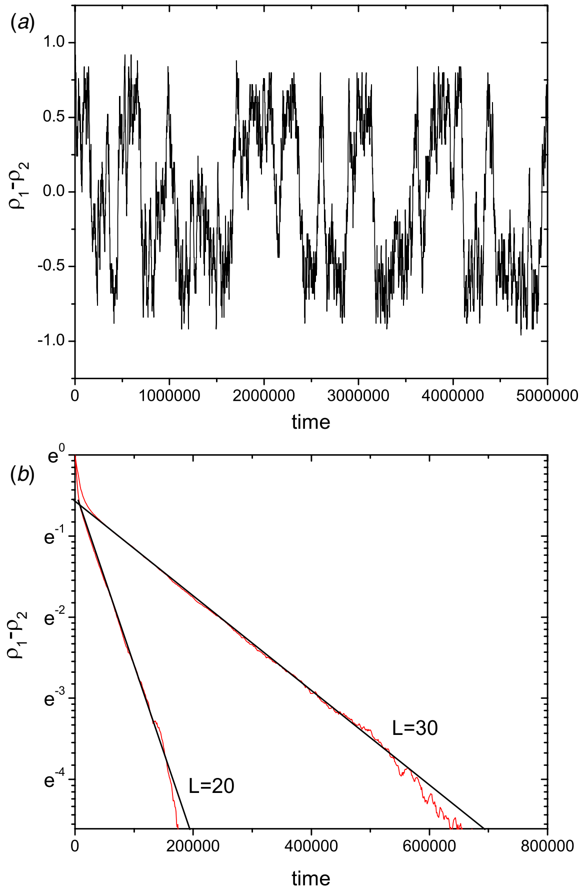

Figure 7. (*a*) Time evolution of the density difference between segments II and IV in an asymmetric phase with $L = 25$. (*b*) Decay of averaged density difference between segments II and IV (over 2×10^4 runs). The solid line is the guide for eyes. The parameters value $\alpha = 0.7$, $\beta = 0.2$ and $r = 1$.

From figure 4, we can also see the value of phase boundary λ_2 increases with the increase of r. It means that the phase HL shrinks while the phase LL and the asymmetric phase expand with the increase of r.

3.3. Results analysis

First, we qualitatively explain the observed symmetry breaking in model B with large α and small β using physical arguments of the domain-wall approach [40]. Suppose initially segments II and IV are empty. When particles reach the exit sites of the two segments, the domain wall (i.e., the shock) will form on the two segments and propagate upstream because the removal rate is smaller than the effective entrance rate in the two segments. Due to randomness, one of the domain wall reaches site c first, which leads to the stable HD phase in the segment. On the other hand, a barrier is formed at site c, which leads to a significant decrease of the effective entrance rate in the other segment. Thus, LD phase instead of HD phase exist in the other segment. As a result, the system is found in the symmetry-broken phase with one lattice in the HH phase and the other one in the HL phase.

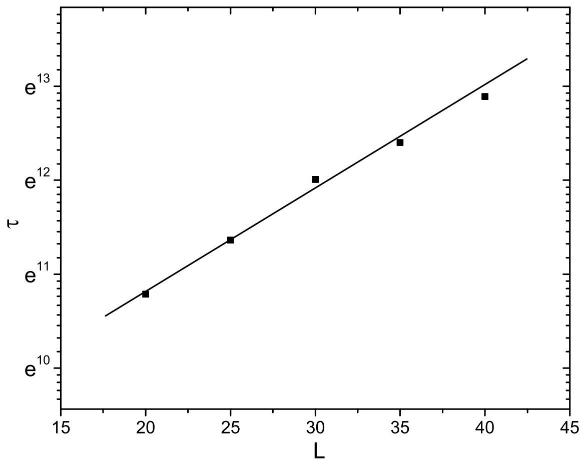

Figure 8. Characteristic flipping time scale τ versus L. The solid lines are the guide for eyes. The parameters value $\alpha = 0.7$, $\beta = 0.2$ and $r = 1$.

Next, the mean-field approach is adopted to analyze stationary states in phases LL and HL. Note that the mean-field analysis is irrelevant to r because correlation is neglected in our mean-field approach. The system is also divided into four segments as shown in figure 1(b). In symmetric phases LL and HL, $\alpha_{\text{eff}} = \frac{\rho_c}{2}$ and $\beta_{\text{eff}} = 1 - \rho_c$.

When the system is in the phase LL, the conditions (5) should be satisfied. From $J_I = J_{II}$ and equation (1), we obtain $\alpha_{\text{eff}} = \frac{\rho_c}{2} = \alpha$, which lead to $\rho_c = 2\alpha$. Substituting $\alpha_{\text{eff}} = \alpha$ and $\beta_{\text{eff}} = 1 - 2\alpha$ into equation (5), we obtain that the system is in LL when the following conditions are satisfied:

$$\begin{cases} \alpha < \frac{1}{3} \\ \alpha < \beta. \end{cases} \tag{13}$$

When the system is in the phase HL, the conditions (9) should be satisfied. From $J_I = (1 - \rho_c)\rho_c = 0.5\rho_c(1 - 0.5\rho_c) = J_{II}$, we obtain $\rho_c = \frac{2}{3}$. Substituting $\alpha_{\text{eff}} = \beta_{\text{eff}} = \frac{1}{3}$ into equation (9), the conditions of existence of HL can be reached:

$$\begin{cases} \alpha > \frac{1}{3} \\ \beta > \frac{1}{3}. \end{cases} \tag{14}$$

From the comparison of equations (13), (14) and figure 4, we know that the approximate stationary solutions are in good agreement with the simulation results when $r = 1$. However, with the decrease of r, the correlation becomes stronger and the mean field results deviate simulation results. Furthermore, the mean-field approach could not be used for spontaneous symmetry breaking phase because the correlation is also strong in asymmetric phase.

4. Model C

4.1. Model rules

Model C also corresponds to vehicle traffic. In model C, there are two types of particles: type 1 enters from site 1 and type 2 enters from site $2L + 2$. The updating rules are as follows: a random site i is chosen during an infinitesimal time interval dt.

- If $i = 1$ (entrance site of lattice 1) and the site is empty, a particle of type 1 is inserted into the site with rate α. If the site is occupied, the particle moves to site $i + 1$ with rate 1 provided the site $i + 1$ is empty. Similarly, if $i = 2L + 2$ (entrance site of lattice 2) and the site is empty, a particle of type 2 is inserted into the site with rate α. If the site is occupied, the particle moves to site $i + 1$ with rate 1 provided the site $i + 1$ is empty.
- If $i = 2L + 1$ (exit site of lattice 1) or $i = 4L + 1$ (exit site of lattice 2) and the site is occupied, the particle is removed with rate β.
- If $1 < i < L+1$ (segment I), or $L+1 < i < 2L+1$ (segment II), or $2L+2 < i < 3L+1$ (segment III), or $3L+2 \leqslant i < 4L+1$ (segment IV) and the site is occupied, the particle moves to site $i + 1$ with rate 1 provided the site $i + 1$ is empty. If site $3L + 1$ (exit site of segment III) is chosen and the site is occupied, the particle moves to site c provided the site c is empty.
- If $i = L + 1$ (site c) and the site is occupied,
  - if the site is occupied by a particle of type 1, then
    * if site c_3 is empty, the particle moves to the site c_3 with rate 1 independent of the status of site c_4,
    * if site c_3 is occupied and site c_4 is empty, the particle moves to the site c_4 with rate p,
  - if the site is occupied by a particle of type 2, then
    * if site c_4 is empty, the particle moves to the site c_4 with rate 1 independent of the status of the site c_3,
    * if site c_4 is occupied and site c_3 is empty, the particle moves to the site c_3 with rate p.

Note that model C with $p = 0$ reduces to model B with $r = 1$.

4.2. Simulation results

The simulation results of model C are described in this section. The phase diagram is shown in figure 9. One can see that three regions are classified as well. When $\alpha < \lambda_3$ and $\alpha < \beta$, the system corresponds to the LL phase: all the four segments are in the LD phase. The corresponding density profiles with $\alpha = 0.2$, $\beta = 0.7$ and different values of p are illustrated in figure 10(*a*). We can see that the bulk densities of all the segments are equal to α under different value of p.

When $\alpha > \lambda_3$ and $\beta > \lambda_3$, the system corresponds to the HL phase: the bulk densities of segments I and III are equal and equal to $1 - \lambda_3$ and that of segments II and IV are also equal and equal to λ_3. The corresponding density profiles are shown in figure 10(*b*). Note that λ_3 decreases with the decrease of p, which means that the HL phase expands with the decrease of p.

When $\beta < \lambda_3$ and $\beta \leqslant \alpha$, the situation depends on p.

- When p is smaller than a threshold $p_{cr} \approx 0.025$, the system corresponds to a symmetry-broken phase, the same as the situation in model B. The corresponding density profiles are shown in figures 10(*c*) and (*d*).
  The density histogram of model C corresponding to the symmetry-broken phase is shown in figure 11. Similar to that of model B, the peak is off the diagonal.
- When $p > p_{cr}$, the system corresponds to a symmetric phase HH if $\beta < \lambda_3$ and $\beta < \alpha$: the bulk densities of all the four segments are equal and equal to $1 - \beta$. See, for example, the density profiles corresponding to $p = 1$ and 0.1 in figures 10(*c*) and (*d*). Furthermore, $\alpha = \beta < \lambda_3$ corresponds to a line of phase transition between phases LL and HH.

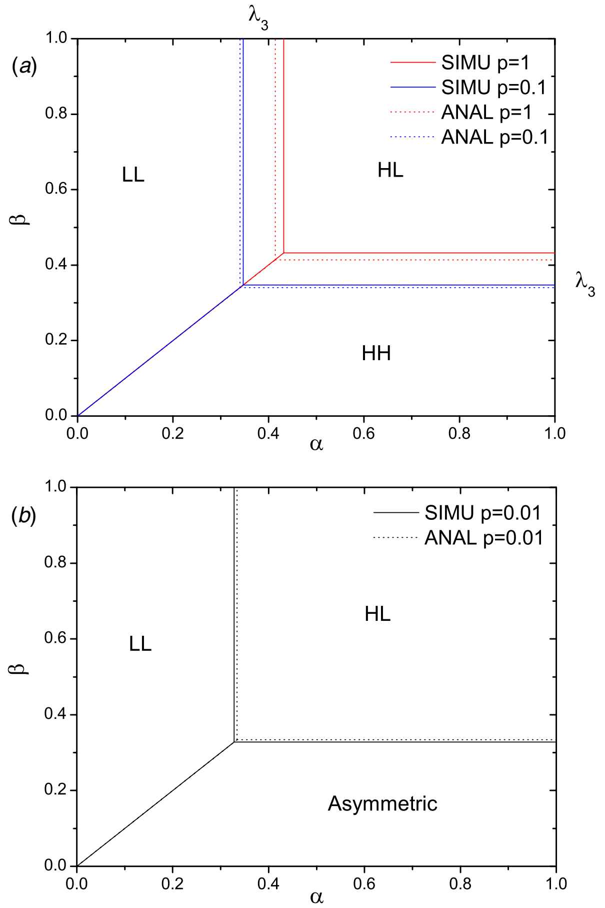

Figure 9. The phase diagram of model C related to α and β. (*a*) $p = 1, 0.1 > p_{cr}$; (*b*) $p = 0.01 < p_{cr}$.

The disappearance of symmetry breaking phenomenon is due to the barrier at site c is broken with the enhancement of randomness.

4.3. Results analysis

In this section, the symmetric phases LL, HH and HL are solved by the mean-field approximation. The same as in models A and B, the expressions of $\alpha_{\rm eff}$ and $\beta_{\rm eff}$ can be obtained:

$$\alpha_{\rm eff} = \frac{\rho_c(p\rho_{c4} + 1)}{2} \qquad \text{and} \qquad \beta_{\rm eff} = 1 - \rho_c. \tag{15}$$

According to equation (1) and $J_I = J_{II}$, for the phase LL, $\alpha_{\rm eff} = \alpha$ and $\rho_{c4} = \alpha$, which leads to $\rho_c = \frac{2\alpha}{p\alpha+1}$. Thus,

$$\alpha_{\rm eff} = \alpha \qquad \text{and} \qquad \beta_{\rm eff} = \frac{(p-2)\alpha + 1}{p\alpha + 1}. \tag{16}$$

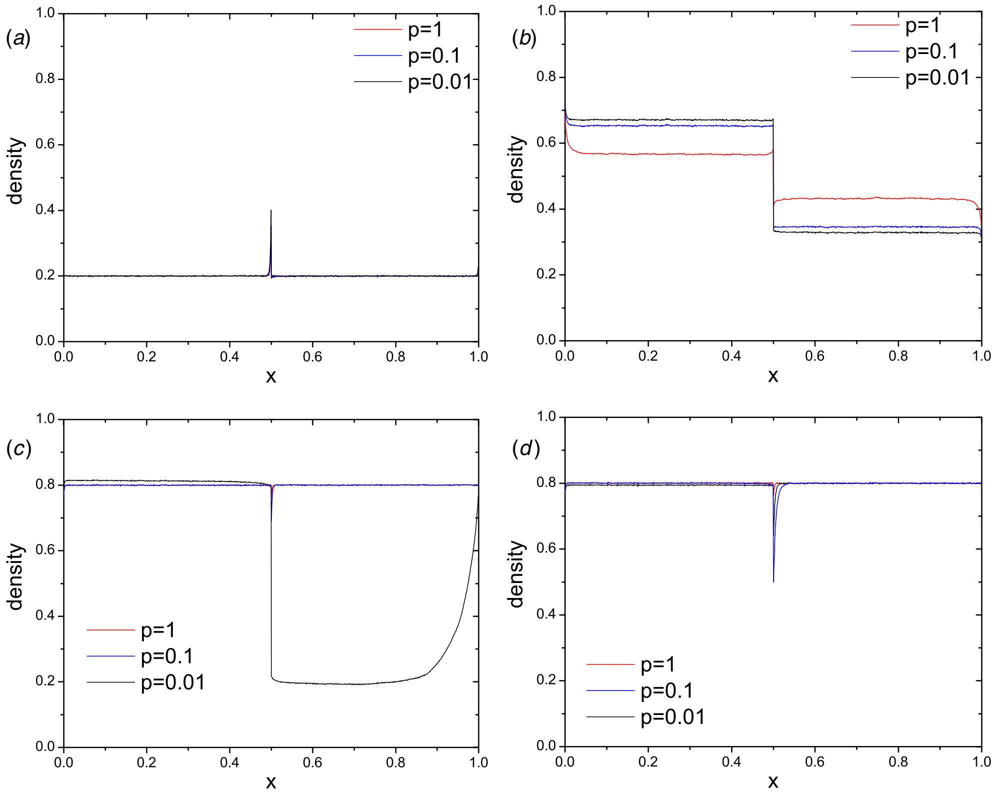

Figure 10. The density profiles of model C corresponding to different phases with different value of p. (*a*) $\alpha = 0.2$ and $\beta = 0.7$; (*b*) $\alpha = 0.8$ and $\beta = 0.7$; (*c*) $\alpha = 0.7$ and $\beta = 0.2$ of lattice 1; (*d*) $\alpha = 0.7$ and $\beta = 0.2$ of lattice 2.

When the system is in the phase LL, the conditions (5) should be satisfied. Substituting equation (15) into equation (5), we obtain that the system is in LL when the following conditions are satisfied:

$$\begin{cases} \alpha < \frac{p-3+\sqrt{p^2-2p+9}}{2p} \\ \alpha < \beta. \end{cases} \tag{17}$$

For the phase HH, we obtain $\beta_{\text{eff}} = \beta$ and $\alpha_{\text{eff}}(1-\rho_{c4}) = \beta(1-\beta)$, which leads to $\rho_c = 1-\beta$ and $\rho_{c4} = \frac{p-1+\sqrt{(1-p)^2-4p(2\beta-1)}}{2p}$. Thus,

$$\alpha_{\text{eff}} = \frac{(1-\beta)(3p-1+\sqrt{(1-p)^2-4p(2\beta-1)})}{4p} \qquad \text{and} \qquad \beta_{\text{eff}} = \beta. \tag{18}$$

When the system is in the phase HH, the conditions (7) should be satisfied. Substituting equation (15) into equation (7), we obtain that the system is in HH when the following conditions are satisfied:

$$\begin{cases} \beta < \frac{p-3+\sqrt{p^2-2p+9}}{2p} \\ \beta < \alpha. \end{cases} \tag{19}$$

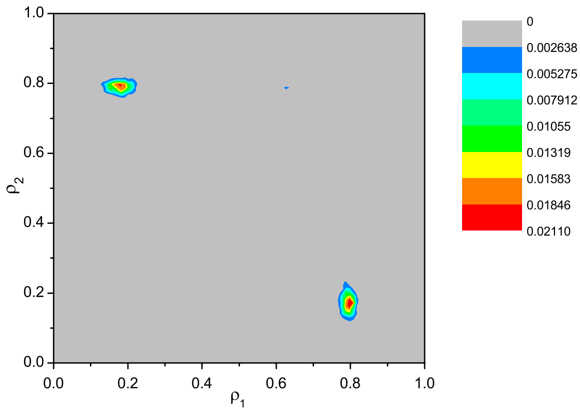

Figure 11. The density histograms of model C corresponding to region II with asymmetric phase. ρ_1 denotes the average density of segment II and ρ_2 denotes the average density of segment IV. $\alpha = 0.7$, $\beta = 0.2$ and $p = 0.01$.

For the phase HL, we obtain $\alpha_{\mathrm{eff}} = \beta_{\mathrm{eff}}$ and $\alpha_{\mathrm{eff}} = \rho_{c4}$, which leads to $\rho_{c4} = 1 - \rho_c$. Substituting the expression of ρ_{c4} into equation (15), we obtain $\rho_c = \frac{p+3-\sqrt{p^2-2p+9}}{2p}$. Thus,

$$\alpha_{\mathrm{eff}} = \beta_{\mathrm{eff}} = \frac{p - 3 + \sqrt{p^2 - 2p + 9}}{2p}. \tag{20}$$

When the system is in the phase HL, the conditions (9) should be satisfied. Substituting equation (15) into equation (9), we obtain that the system is in HL when the following conditions are satisfied:

$$\begin{cases} \alpha > \frac{p-3+\sqrt{p^2-2p+9}}{2p} \\ \beta > \frac{p-3+\sqrt{p^2-2p+9}}{2p}. \end{cases} \tag{21}$$

Obviously, $\lambda_3 = \frac{p-3+\sqrt{p^2-2p+9}}{2p}$. With the decrease of p, the value of λ decreases, which is in good agreement with the simulation results.

5. Conclusion

In this paper, we have presented three different models to investigate the totally asymmetric simple exclusion process on two intersected lattices under open boundaries with random update. Extensive Monte Carlo simulations are carried out. The phase diagrams of all the three models can be classified into three regions. However, differences exist. In model A, the three regions correspond to LL, HH and HL while in model B correspond to LL, spontaneous symmetry-broken phase, HL, respectively. In model C, the corresponding phases of the three regions depends on the value of p. For $p_{cr} < p \leqslant 1$, the three phases are LL, HH and HL and for $0 \leqslant p < p_{cr}$ are LL, spontaneous symmetry-broken phase and HL.

It is intriguing that symmetry breaking phenomena occurs in model B with large α and small β and symmetry breaking will not disappear with different value of r. In model C, however, symmetry breaking phenomena can maintain only when $0 \leqslant p < p_{cr}$. When $p_{cr} < p \leqslant 1$, symmetry breaking disappears. The qualitative explanations of occurrence of symmetry breaking phenomena in model B and its disappearance in model C are presented.

We also investigate the approximate stationary solutions. For model A, bulk densities of all the three phases and the value of λ_1 for transitions are obtained, which are in good agreement with the simulation results. For model B with $r = 1$, the bulk densities of the two symmetric phases and the value of λ_2 for transitions are obtained. It is found that the analytic results are in good agreement with simulation results when $r = 1$. However, with the decrease of r, the mean field results deviate simulation results due to stronger correlation. Moreover, the symmetry-broken phase cannot be solved by the mean-field approach due to the strong correlation in asymmetric phase. And for model C, the value of phase transition λ_3 is calculated.

In our future work, an analytical investigation of the asymmetric phase in models B and C is needed.

Acknowledgments

This work is supported by National Basic Research Program of China (no 2006CB705500), the NNSFC under project nos 10532060, 10404025, 70601026, 10672160, the CAS President Foundation and the Chinese Postdoc Research Foundation (no 20060390179).

References

[1] Derrida B 1998 *Phys. Rep.* **301** 65
[2] Schütz G M 2000 *Phase Transitions and Critical Phenomena* vol 19, ed C Domb and J L Lebowitz (London: Academic)
[3] Blythe R A and Evans M R 2007 *J. Phys. A: Math. Gen.* **40** R333
[4] Macdonald J T, Gibbs J H and Pipkin A C 1968 *Biopolymer* **6** 1
[5] Meakin P, Ramanlal P, Sander L M and Ball R C 1986 *Phys. Rev.* A **34** 5091
[6] Kim J M and Kosterlitz J M 1989 *Phys. Rev. Lett.* **62** 2289
[7] Widom B, Viovy J L and Defontaines A D 1991 *J. Phys. I* **1** 1759
[8] Chou T 1998 *Phys. Rev. Lett.* **80** 85
[9] Shaw L B, Zia R K P and Lee K H 2003 *Phys. Rev.* E **68** 021910
[10] Shaw L B, Kolomeisky A B and Lee K H 2004 *J. Phys. A: Math. Gen.* **37** 2105
[11] Chou T and Lakatos G 2004 *Phys. Rev. Lett.* **93** 198101
[12] Klumpp S and Lipowsky R 2003 *J. Stat. Phys.* **113** 233
[13] Nagel K and Schreckenberg M 1992 *J. Phys. I* **2** 2221
[14] Derrida B, Evans M R, Hakim V and Pasquier V 1993 *J. Phys. A: Math. Gen.* **26** 1493
[15] Schütz G M and Domany E 1993 *J. Stat. Phys.* **72** 227
[16] Lakatos G and Chou T 2003 *J. Phys. A: Math. Gen.* **36** 2027
[17] Chou T and Lakatos G 2004 *Phys. Rev. Lett.* **93** 198101
[18] Mallick K 1996 *J. Phys. A: Math. Gen.* **9** 5375
[19] Evans M R 1997 *J. Phys. A: Math. Gen.* **30** 5669
[20] Kolomeisky A B 1998 *J. Phys. A: Math. Gen.* **31** 1153
[21] Tripathy G and Barma M 1997 *Phys. Rev. Lett.* **78** 3039
[22] Lakatos G, Chou T and Kolomeisky A 2005 *Phys. Rev.* E **71** 011103
[23] Parmeggiani A, Franosch T and Frey E 2003 *Phys. Rev. Lett.* **90** 086601
[24] Popkov V and Peschel I 2001 *Phys. Rev.* E **64** 026126
[25] Popkov V and Schütz G M 2003 *J. Stat. Phys.* **112** 523
[26] Popkov V 2004 *J. Phys. A: Math. Gen.* **37** 1545
[27] Pronina E and Kolomeisky A B 2004 *J. Phys. A: Math. Gen.* **37** 9907
[28] Harris R J and Stinchcombe R B 2005 *Physica* A **354** 582
[29] Mitsudo T and Hayakawa H 2005 *J. Phys. A: Math. Gen.* **38** 3087
[30] Szavits-Nossan J and Uzelac K 2006 *Phys. Rev.* E **74** 051104
[31] Evans M R, Foster D P, Godreche C and Mukamel D 1995 *Phys. Rev. Lett.* **74** 208
Evans M R, Foster D P, Godreche C and Mukamel D 1995 *J. Stat. Phys.* **80** 69
[32] Arndt P F, Heinzel T and Rittenberg V 1998 *J. Stat. Phys.* **90** 783

[33] Clincy M, Evans M R and Mukamel D 2001 *J. Phys. A: Math. Gen.* **34** 9923
[34] Popkov V and Schütz G M 2004 *J. Stat. Mech.* P12004
[35] Levine E and Willmann R D 2004 *J. Phys. A: Math. Gen.* **37** 3333
[36] Erickson D W, Pruessner G, Schmittmann B and Zia R K P 2005 *J. Phys. A: Math. Gen.* **29** L659
[37] Willmann R D, Schütz G M and Grosskinsky S 2005 *Europhys. Lett.* **71** 542
[38] Pronina E and Kolomeisky A B 2007 *J. Phys. A: Math. Gen.* **40** 2275
[39] Ishibashi Y and Fukui M 1996 *J. Phys. Soc. Japan* **65** 2793
[40] Kolomeisky A B, Schütz G M, Kolomeisky E B and Straley J P 1998 *J. Phys. A: Math. Gen.* **31** 6911